Supporting Information

Copper nanoparticle loading and F doping of graphene aerogel enhance its adsorption of aqueous perfluorooctanoic acid

Longfei Liu[1], Naiju Che[1], Shengsen Wang[2], Yanli Liu[1*], Chengliang Li[1*]

[1] National Engineering Laboratory for Efficient Utilization of Soil and Fertilizer Resources, College of Resources and Environment, Shandong Agricultural University, Tai'an 271018, China;

[2] College of Environmental Science and Engineering, Yangzhou University, Yangzhou, 225127, China

Corresponding Authors

*E-mail: chengliang_li11@163.com (C. Li).

*Phone: +86-538-824 5558(C. Li).

*E-mail: yanliliu2013@163.com (Y. Liu).

*Phone: +86-538-824 2250 (Y. Liu).

This document includes the following information:

Part I	1) Synthesis of graphene oxide (GO); 2) Synthesis of fluorinated GO (F-GO); 3) Synthesis of reduced graphene oxide aerogel (rGA); 4) Synthesis of Cu NPs loaded rGA (Cu-rGA); 5) The UPLC analytical method of PFOA; 6) Adsorption kinetic models; 7) Adsorption isotherm models.	
Part II	Figure S1.	The stability of Cu/F-rGA after 48 h equilibrium in (a) different pH (4.11, 7.08, 10.06), (b) ionic strength (10 mM, 50 mM ,100mM) and (c) liquid medium (acetone, chloroform, ethanol).
	Figure S2.	Characterization of Cu/F-rGA. (a and b) Typical SEM of Cu/F-rGA and (c-f) EDS mapping images of Cu/F-rGA.
	Figure S3.	Characterization of (a) Zeta potential of rGA, F-rGA, Cu-rGA and Cu/F-rGA at different equilibrium pH, and (b) FTIR spectrum of Cu/F-rGA before and after PFOA adsorption.
	Figure S4.	The adsorption-desorption behaviors of PFOA on Cu/F-rGA. (a) 1 mM Na_2SO_4, (b) 100 mM Na_2SO_4, (c) ethanol were used as electrolyte solution in the desorption process. (d) Removal capacity of PFOA on Cu/F-rGA within ten times adsorption-desorption and ethanol was as desorption solution.
	Figure S5.	The response surface of the RSM model for the Cu/F-rGA adsorbent
	Figure S6.	The MSE and epoch with different hidden layers
	Figure S7.	(a) The training, test, validation results and (b) performance plot (MSE) under the 4-1-1 ANN topology.
	Figure S8.	ANFIS architecture search
	Figure S9.	Surface output of the ANFIS model for the Cu/F-rGA adsorbent.
	Figure S10.	XPS O1s spectra of Cu/F-rGA (a) before and (b) after PFOA adsorption
	Figure S11.	Artificial neural network architecture.
	Figure S12.	Simplified version of the ANFIS architecture.
Part III	Table S1.	Some typical physic-chemical properties of PFOA
	Table S2.	Physic-chemical properties of GO and different aerogels.
	Table S3.	Adsorption kinetics parameters of PFOA on different aerogels.
	Table S4.	RMSE and R^2 values of test models.
	Table S5.	Parameters of model 3 for the adsorption of PFOA on Cu/F-rGA
	Table S6.	Parameters of the ANN.
	Table S7.	Parameters of the ANFIS.

Part I

1) Synthesis of graphene oxide (GO)

GO was synthesized from natural graphite (325 mesh) via a modified Hummer's method. Briefly, 1 g graphite powder, 3 g $KMnO_4$ and 60 mL concentrated H_2SO_4 solution without mix was respectively introduced in a refrigerator (–18 °C) for 30 min. Then the graphite powder, $KMnO_4$ and concentrated H_2SO_4 solution were successively introduced in a flask (250 mL). The mixture was stirred for 2 h and the temperature was controlled below 20 °C in ice bath. After these steps, the mixture was moved to oil bath at 50 °C and sequentially stirred for 6 hours. The result mixture was slowly poured into a 500 mL beaker with 120 mL of distilled water. The 30 % H_2O_2 solution was dropwise added into the mixture until no bubbling. Finally, the crude product was washed repeatedly with deionized water by centrifuge until the filtrate became neutral. The obtained brown-yellow graphene oxide was saved for use.

2) Synthesis of fluorinated GO (F-GO)

F-GO were synthesized through the one-step hydrothermal process using HF as the fluorination source. Typically, 1 mL HF (40 w.t.%) was added into 35 mL GO (1.0 mg mL^{-1}) aqueous dispersion and this mixture was ultrasonicated for 5 min. Then the dispersion was transferred to a 50 mL Teflon-lined autoclave and sealed. The hydrothermal process was carried out at 120°C for 24 h. After cooling to the room temperature, the prepared F-GO were taken out and immersed into the deionized water to remove the residual acid. The deionized water was changed once 12 h until neutral. The sample was finally vacuum freeze-dried for 48 h.

3) Synthesis of reduced graphene oxide aerogel (rGA)

In a typical fabrication process, 50 mg of GO and 50 mg of sodium dodecyl sulfate (SDS) were dispersed in 10 mL and 1 mL deionized water, respectively, and mixed evenly. Then 100 mg L-ascorbic acid (L-AA) were added into the mixed solution. The template foams were

formed after stirring the mixed solution at 2500 rpm for 10 minutes. Then the template foam was sealed and heated at 80 °C for 12 hours to get hydrogel. The hydrogel was frozen at 18 °C for 4 hours and then thawed at 25 ℃. The hydrogel was washed several times with ethanol to remove unreacted substances. rGA could be obtained by drying the hydrogel at room temperature.

4) Synthesis of Cu NPs loaded rGA (Cu-rGA)

In a typical fabrication process, 16 mg of polyvinylpyrrolidone (PVP) and 80 mg of $CuSO_4 \cdot 5H_2O$ were dissolved into 50 mL deionized water. Then, 5 mg of rGA was soaked in the above mixed solution at 25 °C for 24 hours, and was dried in vacuum drying oven. Finally, the sample was pyrolyzed at 500 °C for 2 h under the protection of Ar, and Cu-rGA aerogel can be obtained after cooling to room temperature.

5) The UPLC analytical method of PFOA

Separation of PFOA was performed using a ultra performance liquid chromatography (UPLC; Ultimate 3000, Dionex Inc., United States of America (USA)) consisting of a autosampler and a LC Pump. Aliquots of 10 μL of purified PFOA-methanol eluents were injected onto a guard column and an analytical column (50 × 2.1 mm Waters BEH C18 column, 1.7 μm pore size, Waters, USA) by the autosampler, and a constant mobile phase of acetonitrile and perchloric acid aquatic solution (pH = 3) was delivered at a flow rate of 0.300 mL/min by the LC Pump. The eluent conditions were 50% acetonitrile and 50% perchloric acid aquatic solution keeping for 5 min at 192 nm. The column temperature were maintained at 50 ℃. In addition, in order to avoid the contamination among different samples, the needle of autosampler was washed and flushed using 90% of methanol (V/V) after every injection.

6) Adsorption kinetic Models

Adsorption kinetics data were simulated by pseudo-first-order kinetics model, pseudo-second-order kinetics model, intra-particle diffusion model and Boyd model, and depicted by Eq. (2), (3), (4) and (5), respectively.

Pseudo-first-order model: $q_t = q_e(1-e^{-k_1 t})$ (1)

Pseudo-second-order model: $q_t = \frac{t}{\frac{1}{k_2 q_e^2} + \frac{t}{q_e}} = \frac{t}{\frac{1}{v_0} + \frac{t}{q_e}}$ (2)

Intra-particle diffusion model: $q_t = K_i t^{1/2} + L$ (3)

Boyd model: $B_t = -0.4977 - \ln(1-\frac{q_t}{q_e})$ (4)

where q_e (mg g^{-1}) and q_t (mg g^{-1}) are the amounts of contaminants adsorbed on the adsorbents at equilibrium and a given time t (min), respectively. k_1 (min^{-1}) and k_2 (g mg^{-1} min^{-1}) are the adsorption rate constants of the pseudo-first-order model and the pseudo-second-order model, respectively. v_0 (μg min^{-1} g^{-1}) is the initial adsorption rate; K_i (mg g^{-1} $min^{-1/2}$) is the overall diffusion constant for the sorption, and L (mg g^{-1}) is the intercept of the vertical axis; B is $\pi^2 D_i \cdot r^{-2}$ (D_i is the effective diffusion coefficient of the adsorbate and r is the radius of adsorbent particles hypothesized to be spherical).

7) Adsorption isotherm Models

Adsorption data of PFOA onto tested adsorbents were analyzed by Langmuir and Freundlich models, where exhibited adsorption characteristics. Therefore, two isotherm models are expressed as following.

Langmuir model: $q_e = \frac{q_m b C_e}{1 + b C_e}$ (5)

Freundlich model: $q_e = K_F C_e^{\frac{1}{n}}$ (6)

where q_e (mg g^{-1}) is the solid-phase concentration, C_e (mg L^{-1}) is the solution concentration, q_m (mg g^{-1}) is the maximum adsorption capacity, b is Langmuir constant, K_F ($mg^{(1-1/n)}$ $L^{1/n}$ g^{-1}) and n are the Freundlich adsorption constants.

Part II

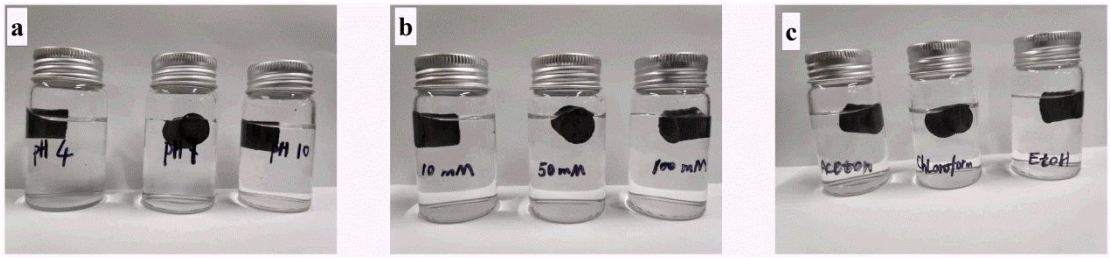

Figure S1. The stability of Cu/F-rGA after 48 h equilibrium in (a) different pH (4.11, 7.08, 10.06), (b) ionic strength (10 mM, 50 mM ,100mM) and (c) liquid medium (acetone, chloroform, ethanol).

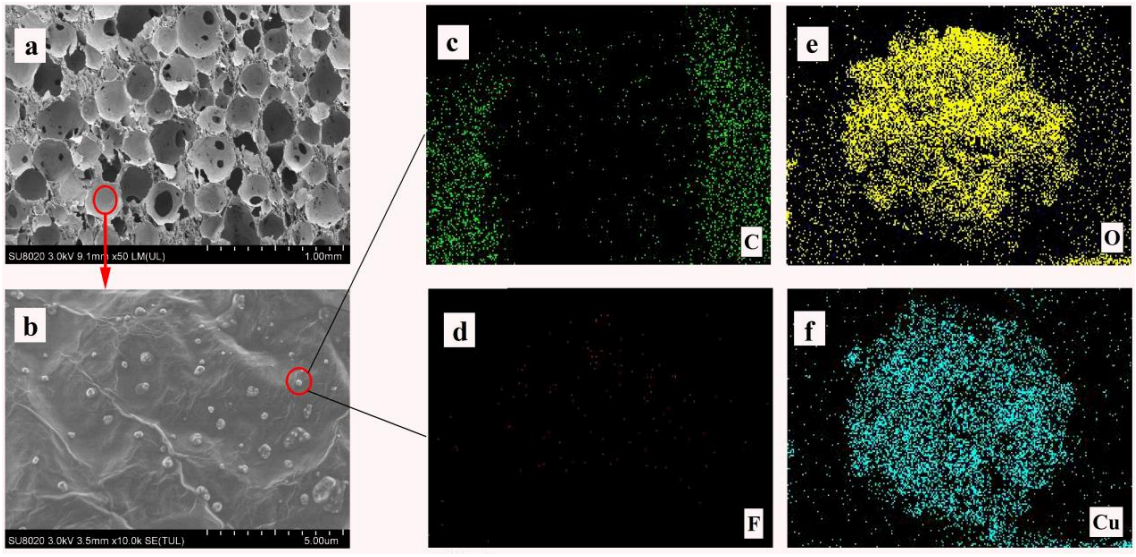

Figure S2. Characterization of Cu/F-rGA. (a and b) Typical SEM of Cu/F-rGA and (c-f) EDS mapping images of Cu/F-rGA.

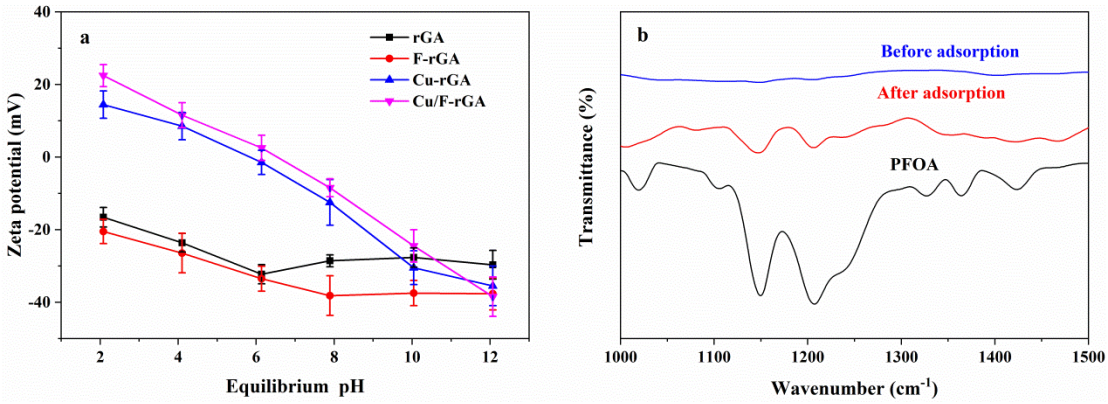

Figure S3. Characterization of (a) Zeta potential of rGA, F-rGA, Cu-rGA and Cu/F-rGA at different equilibrium pH, and (b) FTIR spectrum of Cu/F-rGA before and after PFOA adsorption.

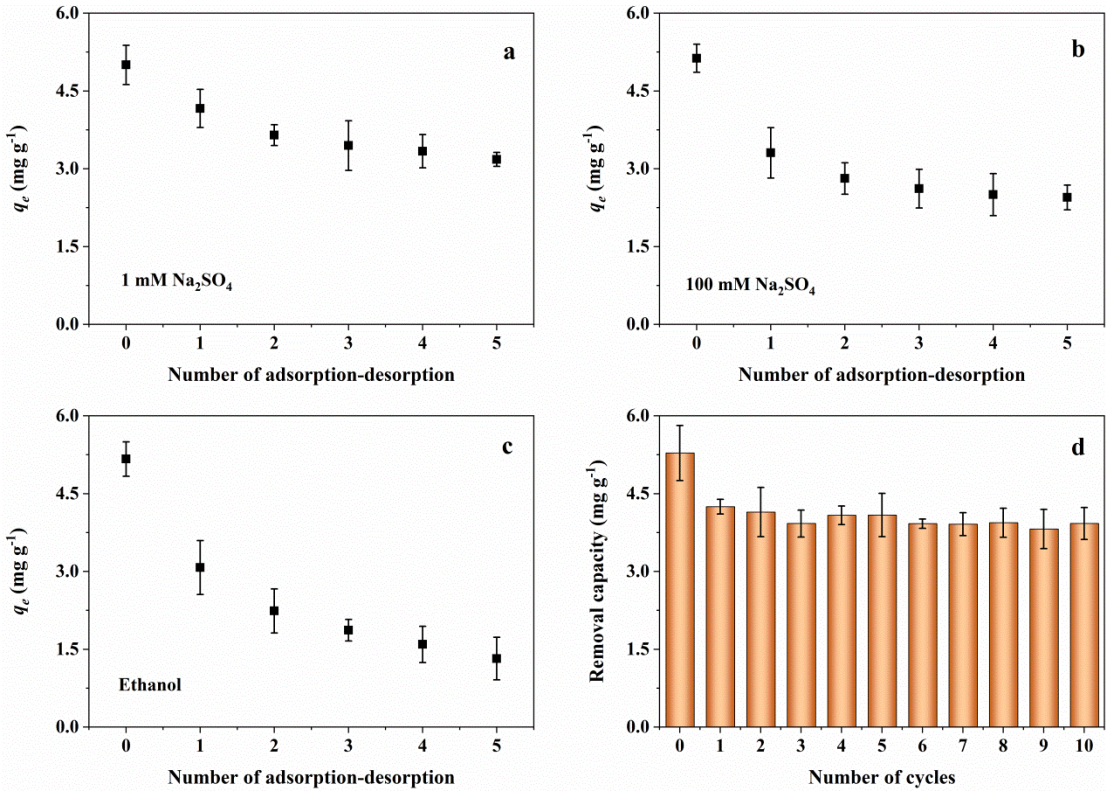

Figure S4. The adsorption-desorption behaviors of PFOA on Cu/F-rGA. (a) 1 mM Na_2SO_4, (b) 100 mM Na_2SO_4, (c) ethanol were used as electrolyte solution in the desorption process. (d) Removal capacity of PFOA on Cu/F-rGA within ten times adsorption-desorption and ethanol was as desorption solution.

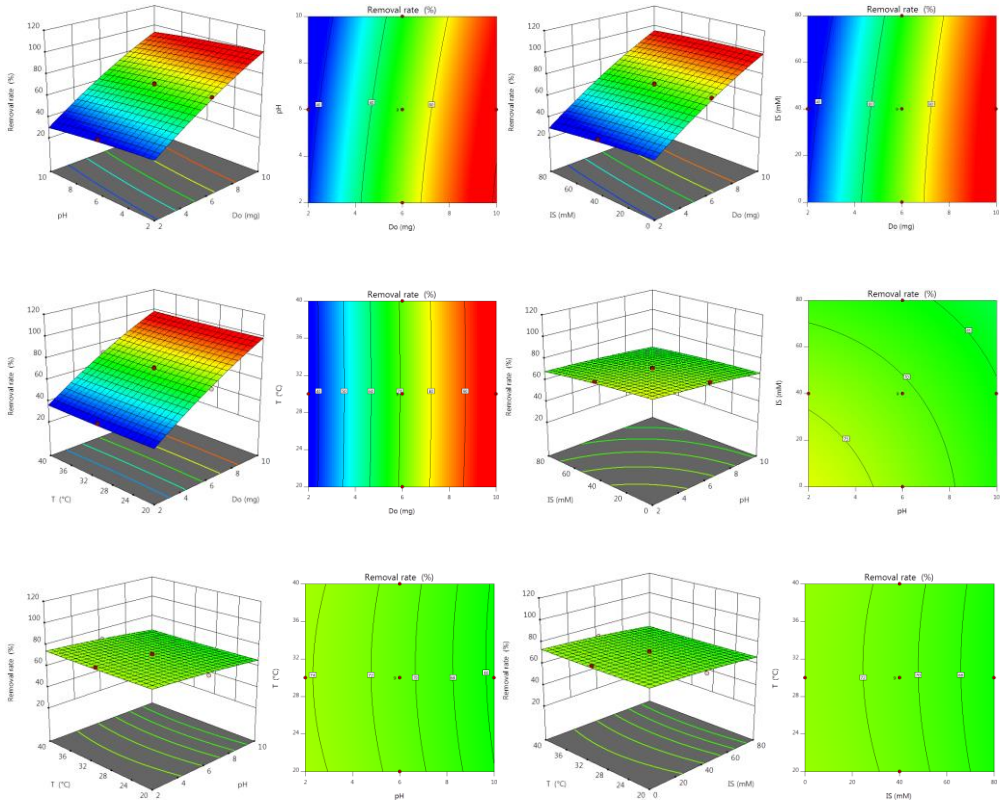

Figure S5. The response surface of the RSM model for the Cu/F-rGA adsorbent

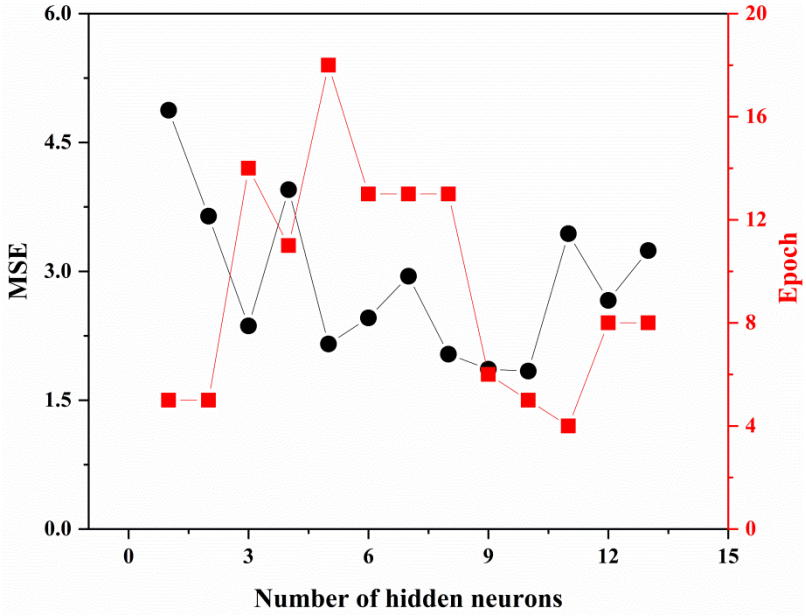

Figure S6. The MSE and epoch with different hidden layers

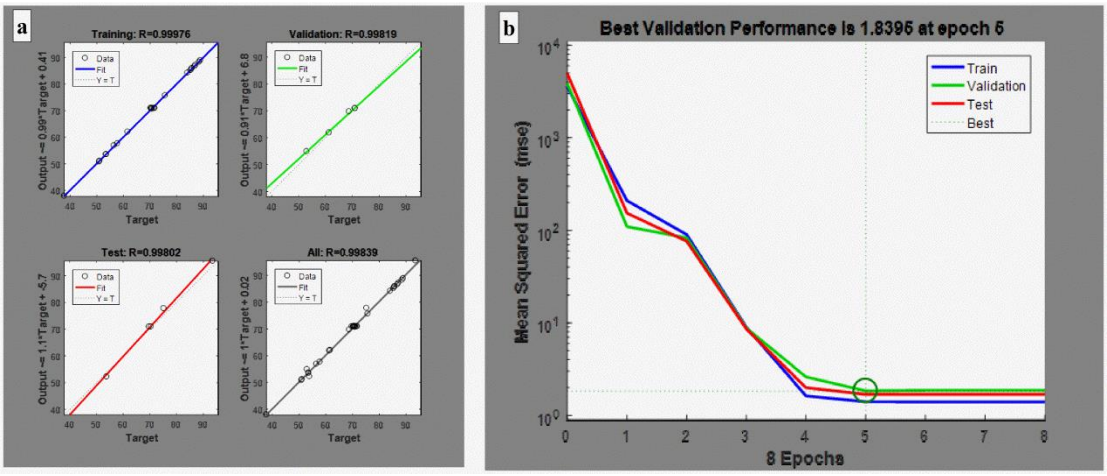

Figure S7. (a) The training, test, validation results and (b) performance plot (MSE) under the 4-1-1 ANN topology.

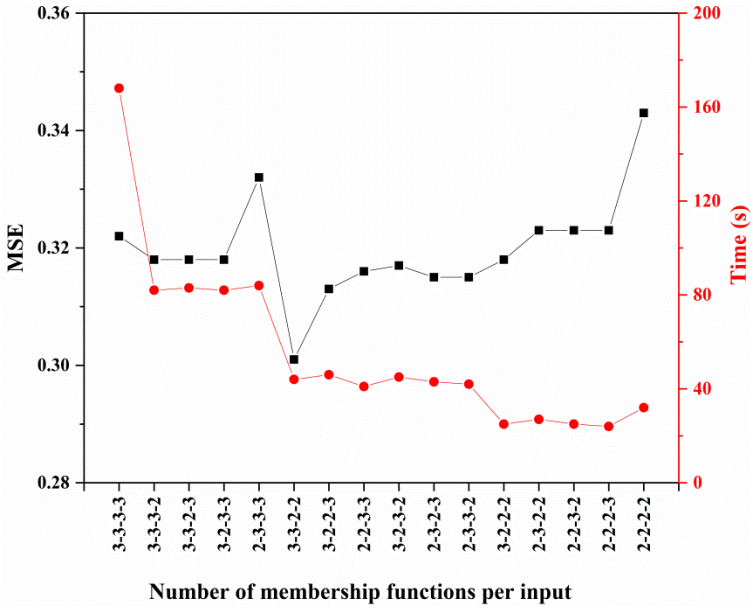

Figure S8. ANFIS architecture search.

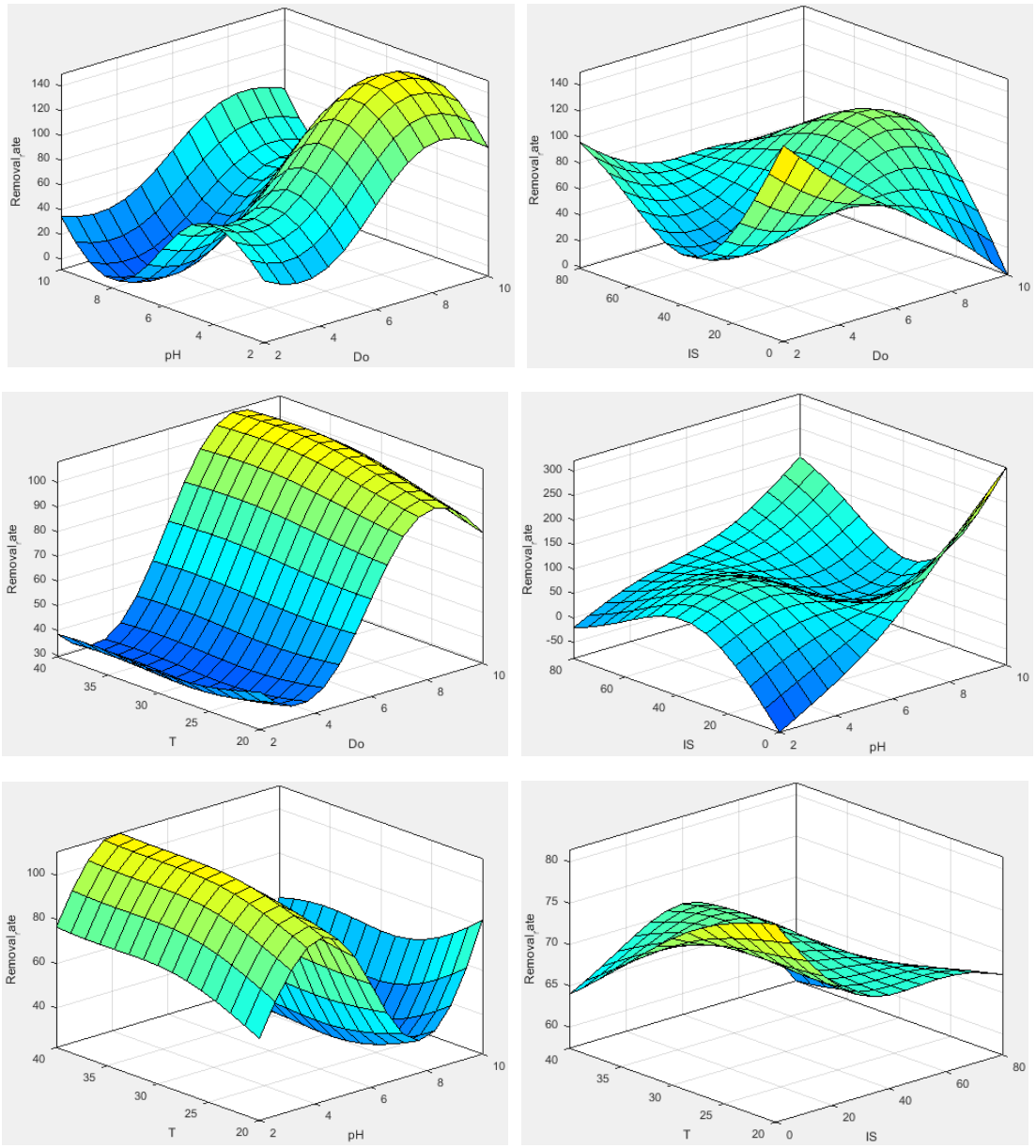

Figure S9. Surface output of the ANFIS model for the Cu/F-rGA adsorbent.

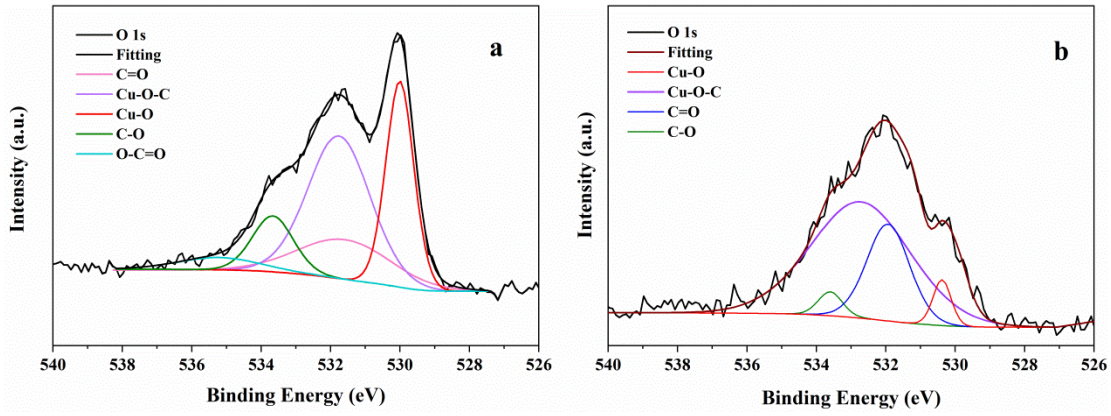

Figure S10. XPS O1s spectra of Cu/F-rGA (a) before and (b) after PFOA adsorption.

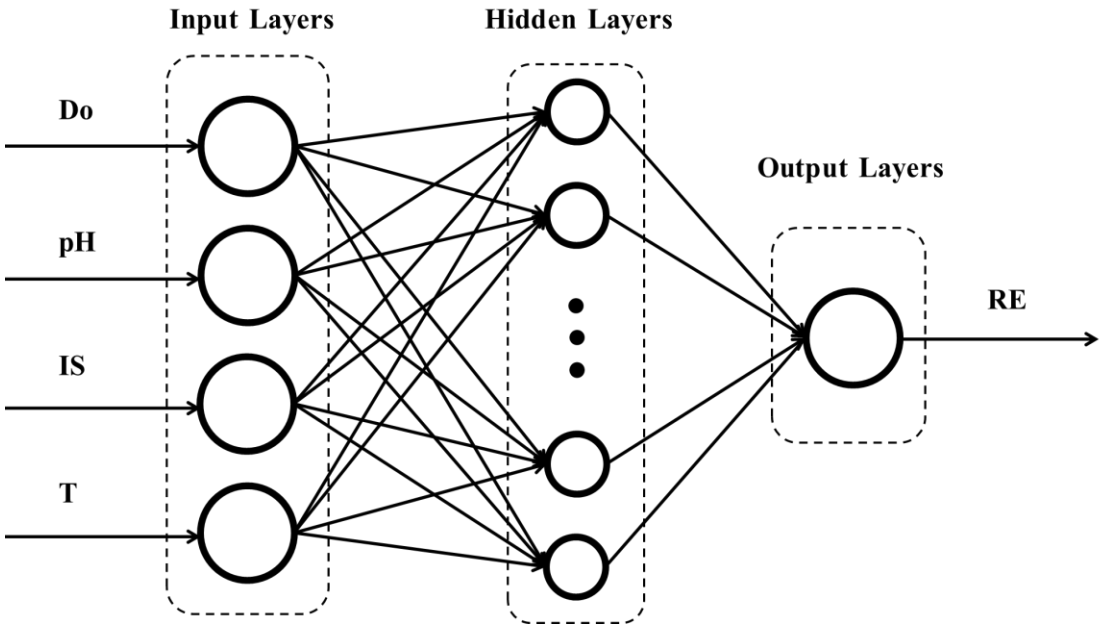

Figure S11. Artificial neural network architecture.

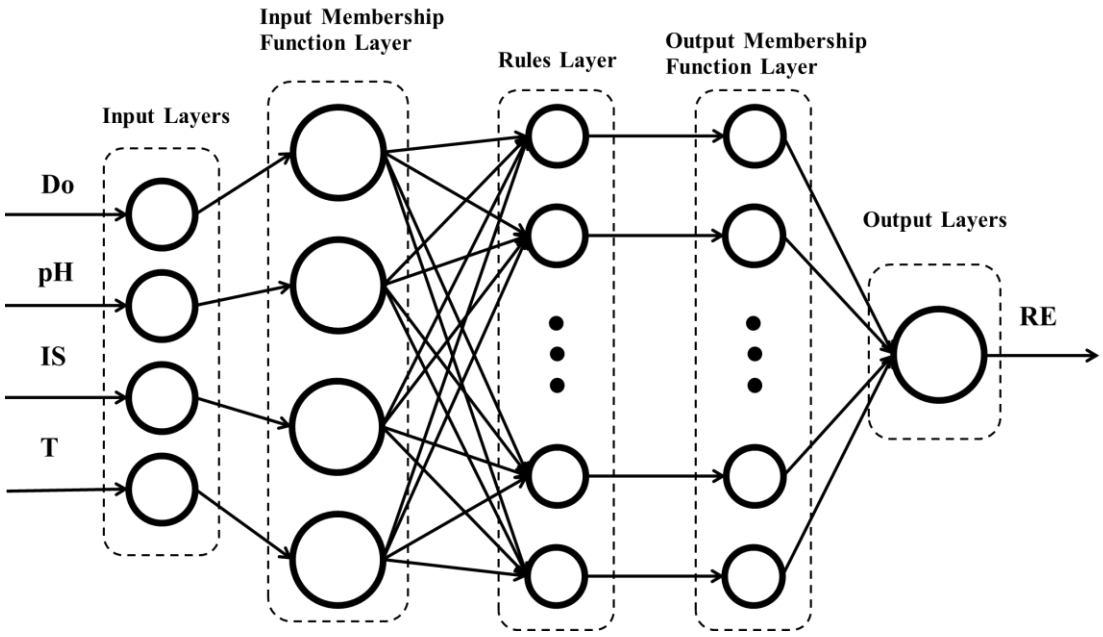

Figure S12. Simplified version of the ANFIS architecture.

ɔle S1. Some typical p hysic-chemical propert ies of PFOA

Chemical	Molecular formula	Structure	Molecular weight (g mol^{-1})	pK_a	Molecular size (nm)	Solubility (g L^{-1})	Melting point (°C)	Boiling point (°C)	Vapor pressure (mm Hg)	log K_{ow}	CMC (g L^{-1})
PFOA	$C_7F_{15}COOH$	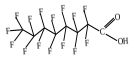	414.07	-0.5	1.2(length)/0.35(diameter)	3.4	45–50	189–192	0.525 (25 °C)	1.92	15.70

ɹ: negative log -transformed acid dissociation constant;

[C: critical micelle concentration;

ɾ: Octanol -Water Partition Coefficient.

ɛerence:

EPA, 2014. Emerging contaminants perfluorooctane sulfonate (PFOS) and perfluorooctanoic acid (PFOA).

3. Deng, Q. Y. Zhang, Y. Nie, H. R. Wei, B. Wang, J. Huang, G. Yu, B. S. Xing, Sorption mechanisms of perfluorinated compo unds
ɛarbon nanotubes, Environ. Pollut. 168 (2012) 138 –144.

Table S2. Some physic-chemical properties of GO and different aerogel.

Adsorbent	SSA_{BET} ($m^2\ g^{-1}$)	PV_{BJH} [a] ($cm^3\ g^{-1}$)	PW_{DFT} [b] (nm)	Ash [c] (%)	Elemental content [d] (%)			
					C	O	F	Cu
GO	286.75	0.18	1.04	0.37	76.45	23.55	–[e]	–
rGA	188.92	1.87	1.54	0.52	85.13	14.87	–	–
F-rGA	203.08	2.36	2.17	0.86	83.24	14.89	1.87	–
Cu-rGA	151.65	1.38	3.83	8.44	78.57	13.18	–	8.25
Cu/F-rGA	133.49	1.19	4.18	8.08	77.58	12.25	2.63	7.54

[a] Pore volume were calculated by Barrett-Joyner-Halenda model;

[b] Average pore width were calculated by Density Functional Theory model;

[c] Ash content was measured by heating the adsorbents at 950°C for 5 h;

[d] C, O, F and Cu elements were measured by XPS survey spectra;

[e] Content was not detected.

Table S3. Adsorption kinetics parameters of PFOA on GO and aerogels.

Adsobate	Pseudo-first-order model		Pseudo-second-order model		
	k_1 (min^{-1})	r^2	v_0 ($mg\ min^{-1}\ g^{-1}$)	k_2 ($g\ mg^{-1}\ min^{-1}$)	r^2
GO	0.0128	0.9866	0.0645	$8.198 \cdot 10^{-3}$	0.9979
rGA	0.0196	0.9868	0.2915	$5.564 \cdot 10^{-3}$	0.9990
F-rGA	0.0180	0.9866	0.4405	$2.977 \cdot 10^{-3}$	0.9983
Cu-rGA	0.0151	0.9970	0.6623	$1.267 \cdot 10^{-3}$	0.9978
Cu/F-rGA	0.0163	0.9924	0.7813	$1.252 \cdot 10^{-3}$	0.9979

Table S4. RMSE and R^2 values of test models

T (°C)	Langmuir		Freundlich		Model 1		Model 2		Model 3	
	R^2	RMSE	R^2	RMSE	R^2	RMSE	R^2	RMSE	R^2	RMSE
20	0.9987	0.3653	0.9727	1.7314	0.9924	0.3662	0.9972	0.3622	0.9992	0.3458
25	0.9981	0.3529	0.9705	1.6768	0.9957	0.3528	0.9966	0.3584	0.9989	0.3345
30	0.9976	0.4615	0.9603	1.7372	0.9964	0.4612	0.9969	0.4585	0.9984	0.4257
35	0.9964	0.5502	0.9646	1.7405	0.9961	0.5508	0.9959	0.5425	0.9981	0.5109
40	0.9977	0.4244	0.9701	1.5587	0.9973	0.4248	0.9986	0.4227	0.9987	0.4036

The R^2 coefficient determines the least sum of squares of the residuals between experimental and modelling data. The second coefficient is defined by the residual root mean square error (RMSE), which can estimate the standard fault of regression between the experimental data and the fit model.

The standard error estimated by RSME is given by:

$$\mathrm{RMSE} = \sqrt{\frac{\mathrm{RSS}}{m\prime - p\prime}}$$

Where RSS represents the sum of residual squares, p' is an adjustable parameter and finally m' represents the number of points of the experimental isotherm. In other words, if the adsorption model is adequate and the estimated parameters are unbiased, then approximately 95 % of the estimated values should fall within $\pm$ 2RMSE of their true values.

Table S5. Parameters of model 3 for the adsorption of PFOA on Cu/F-rGA.

T(°C)	n	N_M (mg g^{-1})	C_1 (mg L^{-1})	C_2 (mg L^{-1})	N_2
20	0.53	25.51	0.73	3.72	1.51
25	0.73	21.28	0.84	4.07	1.17
30	0.97	17.65	1.03	4.34	0.86
35	1.32	13.42	1.49	4.86	0.72
40	1.41	12.54	1.56	5.18	0.63

Table S6. Parameters of the ANN.

Parameter	Description/value
Algorithm	Levenberg–Marquardt back-propagation
Minimized error function	MRPD
Learning	Supervised
Input layer	No transfer function is used
Hidden layer	Hyperbolic tangent transfer function (tansig)
Output layer	Linear transfer function (purelin)
Number of input neurons	4
Number of hidden neurons	10
Number of output neurons	1

Table S7. Parameters of the ANFIS.

Property	Value/comment
Fuzzy structure	Sugeno-type
Initial FIS for training	Genfis1
MF type	Gaussian (‘*gaussmf*’)
Output MF	Linear
Number of clusters	Auto (default)
Optimization method	Hybrid
Number of input neurons	4
Number of output neurons	1
Training maximum epoch number	500
Initial step size	0.01